HOKKAIDO UNIVERSITY

Title	Significant Differences in Effective Stress Coefficient for Rocks within Elastic Region and Peak and Residual Strengths
Author(s)	Dassanayake, A. B. N.; Fujii, Yoshiaki; Fukuda, Daisuke et al.
Description	ARMS8(2014 ISRM International Symposium): 8th Asian Rock Mechanics Symposium. The theme of the symposium is ‘Rock Mechanics for Global Issues - Natural Disasters, Environment and Energy - ’ . 14-16 October 2014, Sapporo, JAPAN
Citation	Proceedings of the 8th Asian Rock Mechanics Symposium, 8, RP1-4
Issue Date	2014-10-14
Doc URL	https://hdl.handle.net/2115/57338
Type	conference paper
File Information	ARMS8.RP1-4.pdf

Hokkaido University Collection of Scholarly and Academic Papers : HUSCAP

Significant Differences in Effective Stress Coefficient for Rocks within Elastic Region and Peak and Residual Strengths

A.B.N. Dassanayake [a]*, Y. Fujii [a], D. Fukuda [a], and J. Kodama [a]

[a] *Hokkaido University, Sapporo, Japan*
* *abndassanayake@gmail.com* (*corresponding author's E-mail)*

Abstract

The values of the effective stress coefficients (α) for intact and fractured rocks were evaluated for three different rocks by conventional method and compared for peak and residual strengths evaluated by Modified Failure Envelope Method (MFEM), which was developed by the authors.

For Kimachi Sandstone, intact rock α values decreased with confining pressure and varied between 1 and 0.8. α value for fractured rock of the same sandstone was higher than the intact rock, reaching nearly one. α value for peak strength decreased from 0.8 to 0.4 with effective confining pressure under both single and multi stage MFEMs. For residual strength state, α value was between that for the peak strength and that for the intact rock.

For Inada Granite, α value for intact rock decreased with confining pressure from 0.9 to 0.7. α value for fractured rock was higher than that for intact rock and nearly one. Value for peak strength was obtained only by multistage test and decreased from 0.8 to 0.2 with confining pressure. The value for residual strength could not be obtained.

For Shikotsu Welded Tuff, the α value for intact rock slightly decreased from 0.95 to 0.90 with increasing confining pressure. The value for fractured rock was higher than α for intact rock and nearly one. MFEM could not be effectively used to determine the values for peak and residual strengths possibly due to pore collapse.

From the above results, it can be concluded that the multistage MFEM is very effective to obtain the value for peak strength. The choice of coefficient values was proposed for stress analysis and failure evaluation, in intact rock structures or structures in rock mass.

Key words: Effective stress coefficient, Modified Failure Envelope Method, peak strength, residual strength

1. Introduction

Determination of the effect of pore pressure on rock deformation is essential for stability analysis in geotechnical applications such as; underground and surface rock structures, oil and gas production, and sequestration of carbon dioxide (Hu *et al*., 2010). Hence, determination of effective stress coefficient (α) is very important because effective stress governs rock failure, and failure criteria for rock strength are represented by effective stress.

The concept of effective stress was first introduced by Terzaghi (1936) for soil, which is commonly known as Terzagi's Effective Stress Principle. It states that the effect of the total stress σ and pore pressure P_p can be represented by a single parameter, known as effective stress σ' and defined as,

$$\sigma' = \sigma - P_p. \tag{1}$$

Terzarghi's effective stress principle is not always valid for the fluid related rocks. Therefore, effective stress coefficient was suggested by Biot (1955) to modify the effective stress principle as,

$$\sigma' = \sigma - \alpha P_p \tag{2}$$

The α is Biot's effective stress coefficient which denotes the ratio of the area occupied by the fluid to the total area in a cross section of a porous material (Bear, 1972). It is the key parameter that quantifies the contribution of pore pressure to the effective stress. For granular soils, the contact area among grains is very small, thus it is possible to assume that a cross section which is considered is

almost occupied by the fluid. Hence, the corresponding effective stress coefficient (α) approximately equals to 1. Rock masses composed of crystallization or cementation, the grain to grain contact is considerably higher and should not assume that the entire cross section is occupied by the fluids. Consequently, the corresponding effective stress coefficient α will be less than 1.

Biot's effective stress coefficient, (α) is usually calculated from experimental results within the elastic region, based on the poroelasticity theory. Values for peak and residual strengths are important when using α to evaluate rock failure, but α obtained as above does not have to be valid for the strengths.

There are limited investigations have been conducted on the effective stress coefficient for the peak strength, but not to determine α for residual strength of rocks. The proposed Modified Failure Envelope Method (MFEM) to evaluate the effective stress coefficient, (α), for peak and residual strengths of rocks (Dassanayake & Fujii, 2014) based on the failure envelope method (Franquet & Abass 1999) was used for Kimachi Sandstone, Inada Granite and Shikotsu Welded Tuff. Multistage tests were examined to reduce the number of specimens as well as the error caused by differences of mechanical properties between specimens.

In this study, α is also determined by a conventional method under hydrostatic stress state for intact and fractured rock to compare with the values obtained by single and multistage MFEMs. The method of choosing the coefficient values is proposed for elastic stress analysis and failure evaluations for intact rock structures and structures in rock mass.

2. Modified Failure Envelope Method (MFEM)

This method requires constructing a failure envelope on differential stress-effective confining pressure plane for saturated samples tested in a triaxial cell with zero pore pressure first, and then for saturated samples with specific pore pressure values. "Zero pore pressure" means pore pressure was controlled to be zero.

From the first set of tests (with zero pore pressure):

Effective confining pressure = total confining pressure

$$P_c' = P_c \tag{3}$$

From the second set of tests (with varying confining and pore pressure):

$$P'_c = P_c - \alpha P_p \tag{4}$$

Peak differential stress data can be plotted with differential stress against effective confining pressure, assuming that α = 0. Data with pore pressure can be shifted to the left by increasing α from 0 to 1 (Fig. 1).

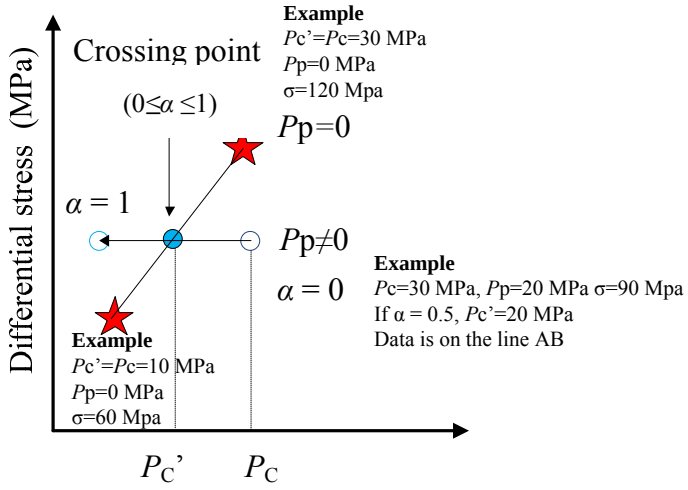

Figure 1. Evaluation of α by the Modified Failure Envelope Method.

The intersecting point can be computed and the α value can be obtained from the effective confining pressure P_C' at that point as,

$$\alpha = \frac{P_C - P_C'}{P_p}. \quad (5)$$

Differential stress was taken as y- axis because it is affected neither by pore pressure nor α value.

3. Specimen and sample preparation

Three rock types were considered in this research, namely Kimachi Sandstone as a medium-hard clastic rock, Inada Granite as a hard crystalline volcanic rock and Shikotsu Welded Tuff as a soft pyroclastic rock.

Firstly, the P-wave velocities of the rock blocks were measured with 140 kHz sensors to determine the anisotropy. Core boring was carried out in the direction of the slowest P-wave velocity to a diameter of 30 mm and cut into a length of 65 mm. End faces of specimens were ground to the length of 60 mm with a parallelism of 2/100.

The specimens were made completely water saturated under a vacuum condition to ensure that all pore spaces were filled with pore fluid because the saturation condition is an important factor for the determination of poroelastic properties. Then the specimens were attached to stainless steel end-pieces, having a central hole for water seepage, and silicone sealant was coated on the specimen. The specimens with the end-pieces were jacketed with heat shrinkable tube to isolate from confining water and it was saturated with distilled water for 24 hours.

4. Experimental procedure

4.1 Single stage triaxial tests

The jacketed sample was set in the ultra compact triaxial cell (Alam *et al*., 2014). After completing the experimental set up (Fig. 2a), axial stress, confining pressure and pore pressure were introduced successively up to the target values (Fig. 2b). Then confining pressure and pore pressure were kept constant while axial compression was introduced at a constant axial strain rate of 10^{-5} s^{-1} (0.036 mm/min) until the axial strain reached to 5%. All the experiments were carried out under a constant temperature of 295K.

4.2 Multistage triaxial tests

Only two samples were required per each rock type for the multi-stage triaxial test. One sample was tested with zero pore pressure using the modified multistage triaxial test (Youn & Tonon, 2010) which is a slight modification of ISRM suggested method (Kovari *et al*., 1983). The confining pressure was increased stepwise to 2 MPa, 5 MPa, 10 MPa and 15 MPa. After confining pressure was introduced successively up to the 1st target value (2 MPa), axial compression was introduced at a constant axial strain rate of 10^{-5} s^{-1} (0.036 mm/min) till it reach for the first imminent failure point. After the first imminent failure point, the differential stress was released completely (Youn & Tonon, 2010) and the confining pressure was hydrostatically increased to the next level (Fig. 2c), after which the differential stress was increased to the second imminent failure point, and so on. The imminent failure point was defined by the region of the stress–axial strain curve where the tangent modulus approaches zero. The second sample was tested by applying non-zero pore pressure, where, confining pressure and pore pressure were introduced successively up to the 1st target value (15 MPa and 14 MPa) and, axial compression was introduced at the same strain rate till it reach for the 1st imminent failure point. After the first imminent failure point, pore pressure was reduced to the next level while maintaining a constant confining pressure of 15 MPa and introduced the axial stress to the second imminent failure point (Fig. 2d). This procedure was repeated for 6 steps with reducing pore pressure of 12 MPa, 10 MPa, 8 MPa, 5 MPa, 1 MPa, and 0 MPa.

Before plotting the peak differential stresses for second sample (PDS_2), the stresses were corrected to reduce the variation in strength between specimens, by;

$$PDS_2' = \frac{PDS_1^0}{PDS_2^0} \times PDS_2 \quad (6)$$

Where, PDS_i^0 denotes peak differential stress of i-th specimen under zero pore pressure (Fig. 3). Reduction of pore pressure to 0 MPa is very important to enable this correction.

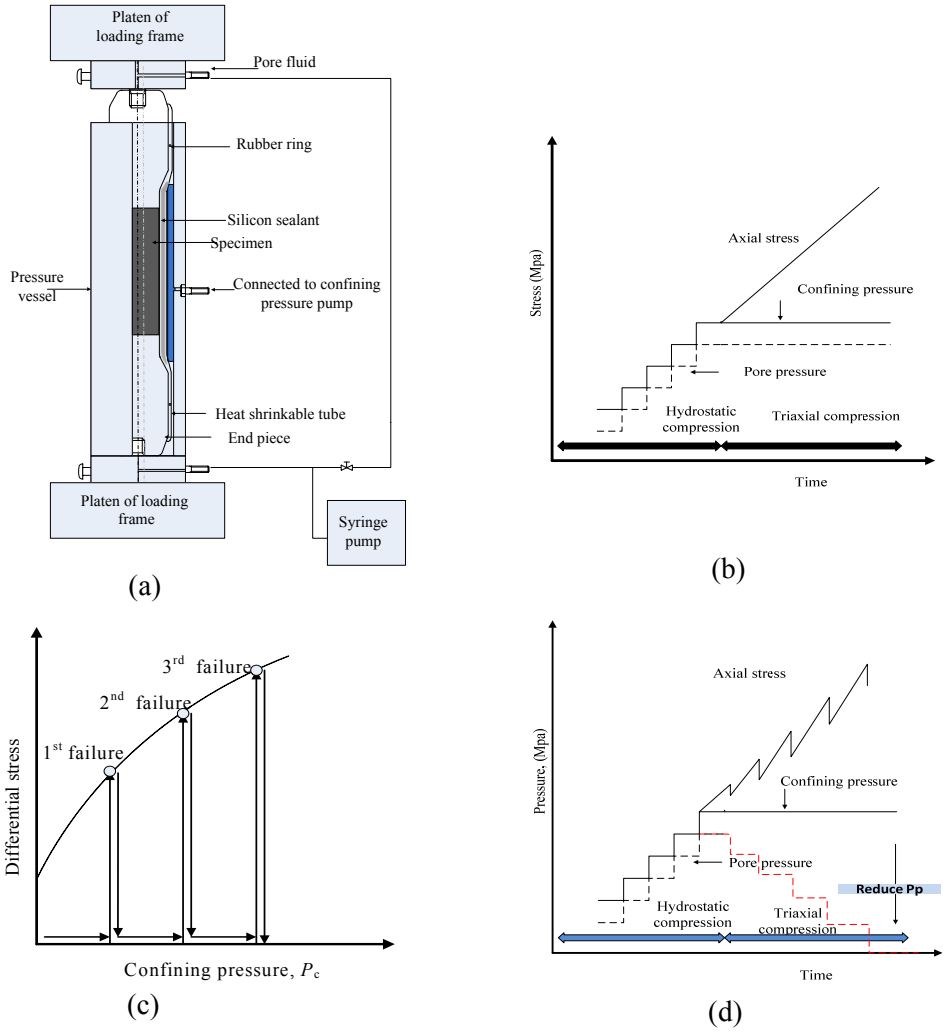

Figure 2. Experimental setup and stress paths of single and multi-stage triaxial tests. a) Experimental setup with ultra compact triaxial cell. b) Procedure to reach the target confining pressure, pore pressure and compression phase of single stage triaxial test. c) Stress paths of multi-stage triaxial test with zero pore pressure. d) Stress paths of multi-stage triaxial test with pore pressure.

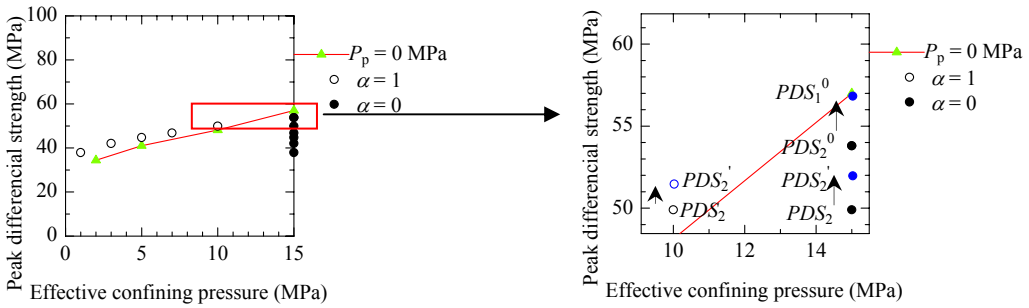

Figure 3. Correction for peak differential stress for Kimachi Sandstone.

4.3 Hydrostatic test for intact rock specimens

In hydrostatic experiments, specimens were exposed to an increased stress state with an isotropic stress field. Two tests per each rock type were required, to determine the bulk modulus of rock, K as a function of effective confining pressure and the bulk modulus of solid matrix (mineral grains), K_s (Hu *et al*., 2010).

The sample preparation was same as the procedure explained in section 3 except the two cross-type strain gauges were attached to the specimen to measure axial and lateral strains in hydrostatic tests. The bulk modulus of rock; K was evaluated by a drained hydrostatic compression test (Hu *et al*., 2010, Makhnenko & Labuz, 2013). In this test, hydrostatic stress was increased stepwise up to 15 MPa, in drained condition with zero pore pressure to determine the bulk modulus, K, of rock (Fig. 4a). The volumetric strain was calculated by axial strain ε_a and lateral strain ε_l as $\varepsilon_v = \varepsilon_a + 2\varepsilon_l$. Bulk modulus, K, was calculated from the volumetric strain curve (Fig. 5) by,

$$K = \left(\frac{\Delta P_c}{\Delta \varepsilon_v} \right)_{\Delta P_p = 0} \tag{7}$$

Where;
ΔP_c= Hydrostatic stress increment
$\Delta \varepsilon_v$= Volumetric strain increment
ΔP_p= Pore pressure increment

In the second hydrostatic test, hydrostatic stress and pore pressure were increased stepwise up to 15 MPa simultaneously with equal increments ($\Delta P_c = \Delta P_p$) keeping $P_p = P_c$ - 1 (MPa) (Fig. 4b) to determine the bulk modulus of solid matrix, K_s of a particular rock type (Hu *et al*., 2010). After determination of volumetric strain, K_s was calculated from the linear phase of the volumetric strain curve (Fig. 6) by,

$$K_s = \left(\frac{\Delta P_c}{\Delta \varepsilon_v} \right)_{\Delta P_c = \Delta P_p} \tag{8}$$

According to the relationship between Biot's Coefficient and compressibility properties (Geertsma, 1957, Biot & Wills, 1957 and Nur & Byerlee, 1971), Biot's Coefficient can be determined by,

$$\alpha = 1 - \frac{K}{K_s} \tag{9}$$

4.4 Hydrostatic test for fractured rock specimens

Bulk modulus of solid matrix, K_s has been measured in advance for intact rock specimen. In order to evaluate Biot's effective stress coefficient for fractured rock, bulk modulus of fractured rock should be determined.

The fractured rock specimens were produced from intact rock samples after breaking them in standard triaxial compression tests with 2 MPa confining pressure and 1 MPa pore pressure, respectively. When samples reached to its residual state, axial loading was stopped and, the differential stress was released completely. Then, the hydrostatic stress was increased stepwise up to 15 MPa, under drained condition with 1 MPa constant pore pressure, to determine the bulk modulus of fractured rock, K_f.

$$\Delta \varepsilon_v = \frac{\Delta V}{V} + \frac{\Delta P_c}{K_s} \tag{10}$$

$$K_f = \left(\frac{\Delta P_c}{\Delta \varepsilon_v} \right)_{\Delta P_p\text{-constant}} \tag{11}$$

Where;
ΔV = Water drainage
V = Specimen volume
K_f = Bulk modulus of fractured rock

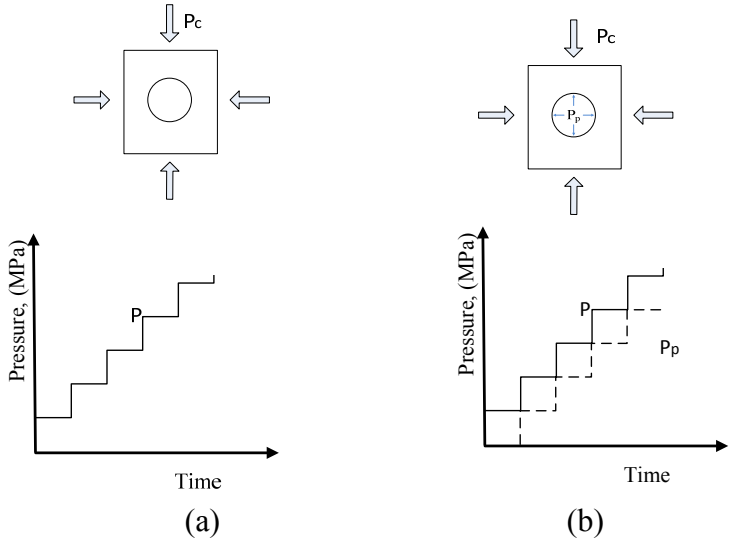

Figure 4. Stress paths of hydrostatic compression tests a) with zero pore pressure: $P_p = 0$. b) with non-zero pore pressure: $\Delta P_c = \Delta P_p$.

5. Results

5.1 Kimachi Sandstone

In drained hydrostatic compression test with zero pore pressure, the bulk modulus of intact rock increased with increasing hydrostatic pressure (Fig. 5a) due to closure of microcracks and elliptical pores. Consequently, α decreased with confining pressure and ranged between 1 and 0.8 (Fig. 7a). α values for fractured rock by hydrostatic tests were higher than α for intact rock and nearly one (Fig. 7a).

α value for peak strength decreased from 0.8 to 0.4 with increasing effective confining pressure under both single and multi stage MFEMs (Fig. 8a). The values were significantly lower than those for intact rock under hydrostatic condition. For residual strength, α value was regulated between that for the peak strength and that for the intact rock (Fig. 8a).

5.2 Inada Granite

Similar to the Kimachi Sandstone, in drained hydrostatic compression test with zero pore pressure, the bulk modulus of Inada Granite intact rock increases with increasing hydrostatic pressure (Fig. 5b) due to closure of microcracks and as a consequence α decreased with confining pressure from 0.9 to 0.7 (Fig. 7b). The results show rather large variation in α, which may have caused due to small strain. α values for fractured rock by hydrostatic tests were higher than α for intact rock and nearly one (Fig.7b).

Value for peak strength by single stage MFEM slightly scatters around 1 (Fig. 8b). In contrast, at higher effective confining pressures 10 - 15 MPa, α value showed a higher variation with large deviations from 1 (Fig. 8b). In multistage triaxial test, the test steps were stopped just before yielding due to the brittleness of the rock. The results showed that α for peak strength decreased from 0.8 to 0.2 with increasing effective confining pressure (Fig. 8b). For residual strength, the behavior of α value with effective confining pressure showed almost same as the peak strength (Figs. 8b).

5.3 Shikotsu Welded Tuff

Almost linear response was observed in volumetric strain versus hydrostatic pressure (Fig. 5c), in drained hydrostatic compression test with zero pore pressure. This is caused by the microstructure of the rock, namely there are few microcracks and number of large circular pores which never cause closure (Fig. 9). As a result, almost constant values for bulk modulus and consequently a constant α values were obtained which ranged between 0.95 and 0.90 (Fig.7c). α values for fractured rock by hydrostatic tests were higher than α for intact rock and nearly one (Fig. 7c).

MFEM could not be used to accurately determine the effective stress coefficient for peak strength through single stage and multistage triaxial tests (Fig.8c). The strength with pore pressure was larger

than that with zero pore pressure in many cases (Fig. 10). This may be caused by an end-cap like failure surface at higher stresses (Dassanayake & Fujii., 2014) due to pore collapse (Zaman *et al*., 1994) by crushing of rock matrix consisting of volcanic glass. The decrease of α value for residual strength with effective confining pressure shows the progress of pore collapse. Poroelasticity itself cannot be applied to this condition.

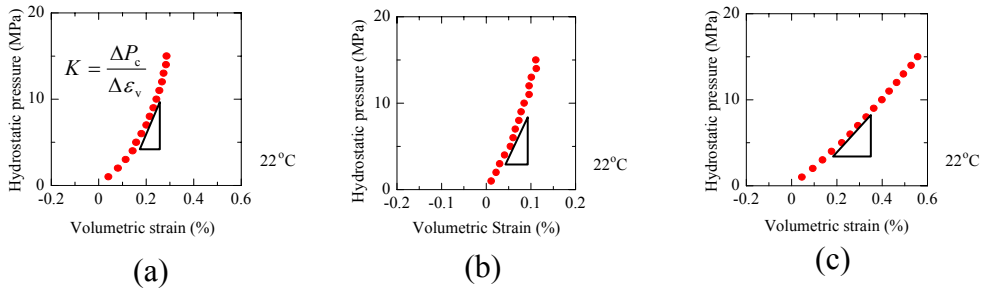

Figure 5. Stress-strain curve in hydrostatic compression test for P_p=0 a) For Kimachi Sandstone b) For Inada Granite c) For Shikotsu Welded Tuff

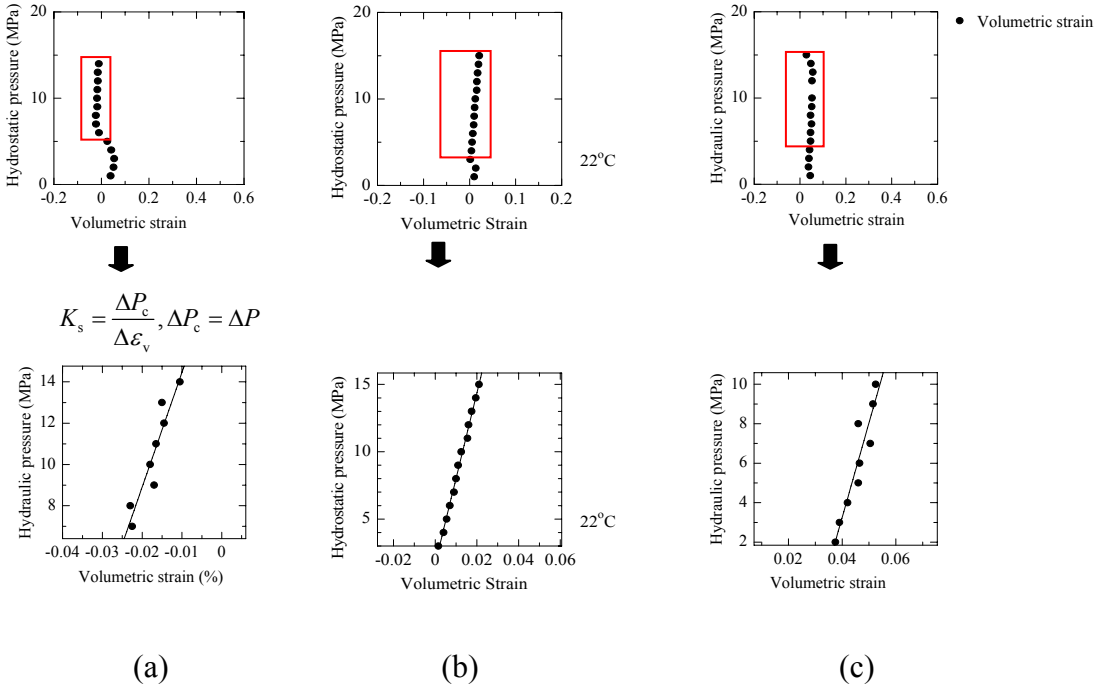

Figure 6. Stress-strain curve in hydrostatic compression test with pore pressure: ΔP_c=ΔP_p. a) For Kimachi Sandstone b) For Inada Granite c) For Shikotsu Welded Tuff

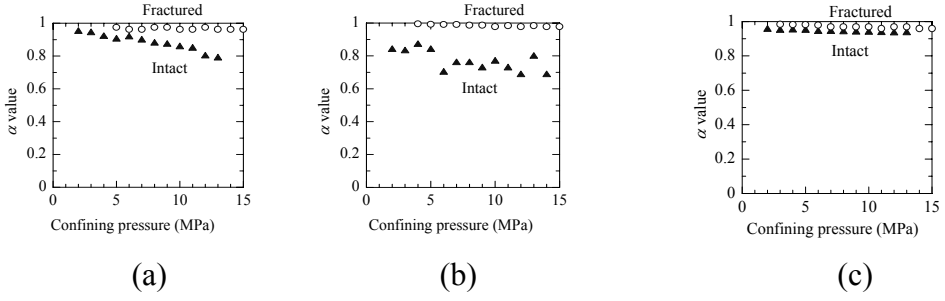

Figure 7. Biot's effective stress coefficient by hydrostatic test for intact and fractured rock specimens of a) Kimachi Sandstone b) Inada Granite and c) Shikotsu Welded Tuff

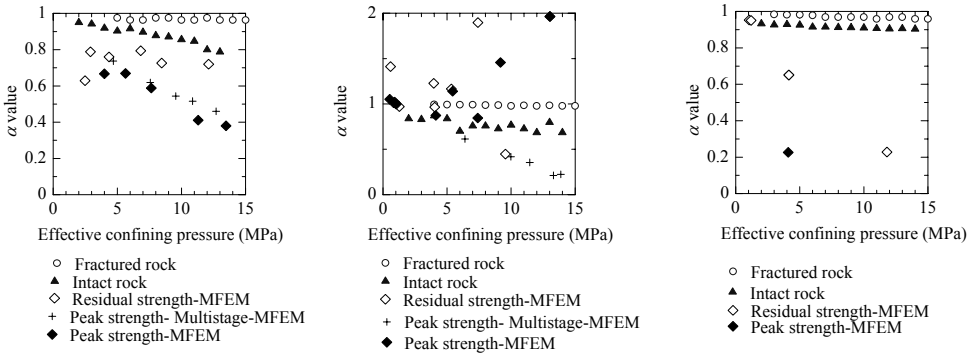

Figure 8. Summary of effective stress coefficients for a) Kimachi Sandstone b) Inada Granite and c) Shikotsu Welded Tuff

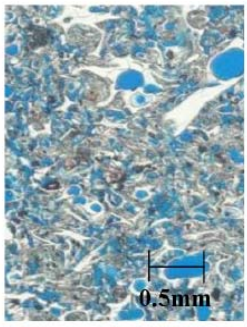

Figure 9 Blue resin-impregnated thin-section of Shikotsu Welded Tuff.

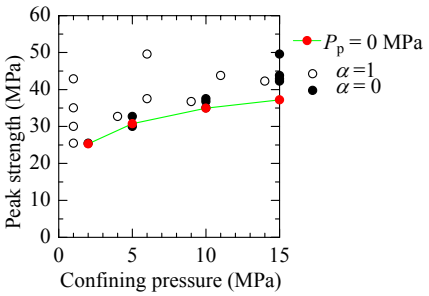

Figure 10 Peak differential stress vs effective confining pressure when $\alpha = 0$ and $\alpha = 1$ for Shikotsu Welded Tuff.

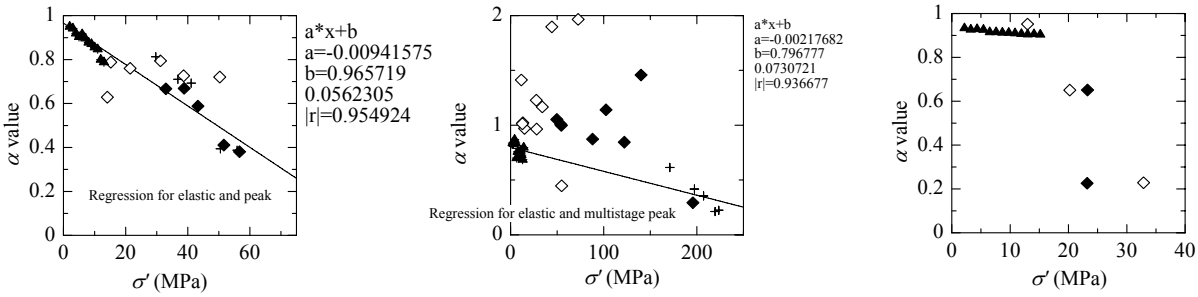

Figure. 11 Effective normal stress vs α for a) Kimachi Sandstone b) Inada Granite and c) Shikotsu Welded Tuff

6. Discussion

6.1 Applicability of MFEM

MFEMs were successfully applied to Kimachi Sandstone. Only multistage MFEM was successful for Inada Granite. MFEM did not give good results for Shikotsu Welded Tuff. From the above results, multistage MFEM is recommended to obtain the effective stress coefficient for peak strength of rocks. The strength correction in the multistage MFEM is particularly effective to obtain results with small scatters.

6.2 Relationship between the coefficient values for intact rock and strengths

α for peak strengths of intact rocks can be plotted almost linearly by taking effective normal stress on the rupture plane as x-axis for Kimachi Sandstone assuming that the rupture plane is inclined by 30º (Fig. 11). The values for residual strength are largely scattered but located around the regression line. This implies that the tedious single stage MFEM to evaluate residual strength could be skipped. The evaluation of the coefficient value does not work well for Inada Granite. However, the evaluation might be possible by allowing the scatter. The values for residual strength could not be obtained due to large scatter but mechanical analysis can be conducted assuming the values are on the line. The evaluation completely does not work for Shikotsu Welded Tuff. From the behavior for the high normal stresses, it is apparent that pore collapse occurred and drastically changed the rock microstructure.

6.3 The selection of the coefficient

For elastic stress analysis of intact rock structures, the coefficient for intact rock can be used and the coefficient value can be evaluated by the hydrostatic test for intact rock as well as using conventional methods.

However, the coefficient for peak strength should be used to evaluate rock failures. The coefficient value can be easily evaluated by multistage MFEM except for rocks which cause drastic structure change due to pore collapse etc. The value was much smaller than that for intact rocks. Combining the coefficient values for intact rock and peak strength by the effective normal stress might enable seamless analyses.

For elastic stress analysis of a structure in rock mass, the coefficient for fractured rock can be used although there is a scale effect problem between rupture planes in a fractured rock and fractures in a rock mass. The coefficient value can be evaluated by hydrostatic test for fractured rock. The test however can be skipped since the value was larger than those for intact rock and was virtually one.

To evaluate rock mass failure, the coefficient for residual strength could be used. This coefficient value can be evaluated by single stage MFEM. The evaluation was successful only for Kimachi Sandstone so far and the value was between that for intact rock and peak strength. The coefficient values for fractured rock and for residual strength could not be related by the effective normal stress which is yet to be solved by further investigations on the coefficient for residual strength.

7. Conclusions

The values of the effective stress coefficients (α) for intact and fractured rock were evaluated for three rock types by rather conventional method and compared to those for peak and residual strengths evaluated by MFEM (Modified Envelope Method) developed by the authors.

For Kimachi Sandstone, α value for intact rock decreased with confining pressure and ranged between 1 and 0.8. α value for fractured rock was higher than that for intact rock and nearly one. α value for peak strength decreased from 0.8 to 0.4 with effective confining pressure under both single and multi stage MFEMs. For residual strength state, α value was between that for the peak strength and that for the intact rock.

For Inada Granite, α value for intact rock decreased with confining pressure from 0.9 to 0.7. α value for fractured rock was higher than that for intact rock and nearly one. Value for peak strength was obtained only by multistage test and decreased from 0.8 to 0.2 with confining pressure. The value for residual strength could not be obtained.

For Shikotsu Welded Tuff, the value for intact rock slightly decreased from 0.95 to 0.90 with confining pressure. The value for fractured rock was higher than α for intact rock and nearly one. MFEM could not be effectively used to determine the values for peak and residual strengths possibly due to pore collapse.

From the results, it can be concluded that the multistage MFEM can be used to obtain the values for peak strength. The way to select the coefficients values were proposed for elastic stress analysis

and failure evaluation for either intact rock structures or structures in rock mass. Development of multistage MFEM for residual strength, data accumulation and deliberate consideration on the scale effects between rupture planes in a fractured rock and fractures in a rock mass will further contribute to reasonable design of rock structures in future.

Acknowledgement

This work was partially supported by KAKENHI (26420840).

References

Alam, A.K.M.B, Niioka, M., Fujii, Y., Fukuda, D., and Kodama, J., (2014). Effects of confining pressure on the permeability of three rock types under compression *International Journal of Rock Mechanics and Mining Sciences* 2014.

Bear, J., (1972). Dynamics of fluids in Porous Media. New York: American Elsevier Publishing Company.

Biot, M.A., (1955). Theory of elasticity and consolidation for a porous anisotropic solid. *J Appl Phys*; 26:182–5.

Biot, M.A. and Willis, D.G., (1957). The elastic coefficients of the theory of consolidation. *ASME Journal of Applied Mechanics*, 24, 594–601

Dassanayake, A.B.N. and Fujii, Y., (2014*)*. Biot's Effective Stress Coefficient of Rocks for Peak and Residual Strengths by Modified Failure Envelope Method*. Proc. of 2014 EUROCK Sympo*

Franquet, J. A.. and Abass, H. H., (1999). Experimental evaluation of Biot's poroelastic parameter - Three different methods, *37th U.S. Symposium on Rock Mechanics (USRMS),* June 7-9 Vail, CO, Balkema, Rotterdam, 349–355.

Geertsma, J., (1957). The effect of fluid pressure decline on volumetric changes of porous rocks: Petroleum Transactions, *AIME*, 210, 331–340.

Hu, D.W. Zhou, H, Zhang, F. and Shao, J.F., (2010). Evolution of poroelastic properties and permeability in damaged sandstone*. International Journal of Rock Mechanics and Mining Sciences*, 47 pp. 962–973

Kovari, K, Tisa, A., Einstein, H.H., and Franklin, J.A., (1983). Suggested methods for determining the strength of rock materials in triaxial compression: revised version. *Int J Rock Mech Min Sci*; 206:283–90.

Makhnenko, R.M., and Labuz, J.F., (2013). Unjacketed bulk compressibility of sandstone in laboratory experiments. *Proceedings of the 5th BIOT Conference on Poromechanics*, Vienna, Austria, 10-12 July 2013, paper No. 304

Nur, A., and Byerlee, J. D., (1971). An exact effective stress law for elastic deformation of rock with fluids: *Journal of Geophysical Research Solid Earth*, 76, 6414–6419

Terzaghi, K., (1936). The shearing resistance of saturated soils and the angle between the planes of shear, *First Int. Conf. Soil Mech*., Vol. 1, Harvard Univ., Cambridge, Mass.:54-56

Youn, H., and Tonon, F., (2010). Multi-stage triaxial test on brittle rock. *International Journal of Rock Mechanics & Mining Sciences* 47: 678–684

Zaman, M., Roegiers, J.C. Abdulraheem, A., and Azeemuddin, M., (1994). Pore collapse in weakly cemented and porous rocks. *J of Energy Resources Tech* 116:97-103.